ROYAL SOCIETY OF CHEMISTRY

PAPER

Check for updates

Evaluation of the performance of different membrane materials for microalgae cultivation on attached biofilm reactors†

Yonggang Zhang, [ID] [a] Rui Ma,[b] Huaqiang Chu,[b] Xuefei Zhou, [ID] [b] Tianming Yao [ID] *[a] and Yalei Zhang [ID] *[b]

Attached microalgae production in wastewater is a promising method to further develop biofilm reactors by reducing economic costs associated with biomass separation and harvesting. However, the reliability of materials to support such adherence needs further investigation. Five common microfiltration membranes were evaluated in this study to assess their influence on the efficacy of harvesting *Chlorella pyrenoidosa*. The material-to-material, algae-to-algae, and algae-to-material interactions were studied based on the Extended Derjaguin, Landau, Verwey, Overbeek (XDLVO) theory. The results showed that *Chlorella pyrenoidosa* was hydrophobic and that the algae particles derived from this algae type tended to agglomerate. Furthermore, the algae–membrane adhesion free energy further validated the accumulation of biomass in the experiments — the cellulose acetate nitrate (CACN) membrane and the cellulose acetate (CA) membrane obtained an optical biomass production of 59.93 and 51.27 g m^{-2}. The presence of these interactions promoted the adhesion of more microalgae particles to the membrane. Moreover, the relationship between the algae–membrane and the distance at which the microalgae approached the membrane surface was simulated. The study indicated that the XDLVO theory could be successfully applied to the mechanism for the adhesion of the attached culture of *Chlorella pyrenoidosa* to the membrane material.

1 Introduction

Microalgae has great potential to be used as a feedstock for the production of bio-products including biodiesel, food additives and other chemical compounds.[1,2] Compared with traditional biofuel, microalgae are becoming increasingly attractive because of their rapid growth rate, high oil content, species diversity, carbon fixation capacity and photosynthetic productivity, as well as their ability to sidestep competition with food products for arable land use. The development of the microalgae industry for biofuels is also effective at reducing global warming and removing pollutants from wastewater.[3,4] Despite the great versatility of microalgae, they have not yet been commercialized due to their high production cost. Currently, microalgae are mainly cultivated in open ponds and photobioreactors as dilute suspensions; however, the extraction of biomass using these methods is expensive. It has been estimated that the cost of harvesting algae accounts for 20–30% of the total operating cost.[5,6]

Newer technologies, such as the semi-dry attached cultivation method, have been proposed to reduce the microalgae harvesting cost. Attachment culture is a method for immobilizing microalgae by adsorption. In this method, the microalgae cells are fixed on the surface of a medium material in the form of a semi-dry biofilm that is separated from the medium. Compared with traditional suspended cultures, attached cultures have higher utilization rates of solar energy, consume less growth media, and are easier to harvest.[7–9] Therefore, attached cultures are expected to achieve an important breakthrough in microalgae culture technology in subsequent years.

Dozens of adherent photo-bioreactors have been reported in recent years, which proves the feasibility of this technology.[10] This type of reactor significantly reduces water and energy consumption and increases the convenience of microalgae collection. However, there are some issues that currently hamper the development of this technology, including selection of the substratum material, optimization of nutrient supply tactics, environmental impact factors, and determination of the mechanism of CO_2 and nutrient mass transfer in the biofilm. These areas need to be further explored before this technology can be successfully applied to the field of algae cultivation and harvesting.[7,10,11] Among these issues, the rational choice of

[a] School of Chemical Science and Engineering, Tongji University, Shanghai 200092, China. E-mail: tmyao@tongji.edu.cn; Fax: +86-21-65985811; Tel: +86-21-65983292

[b] State Key Laboratory of Pollution Control and Resource Reuse, Tongji University, Shanghai 200092, China. E-mail: zhangyalei@tongji.edu.cn; Fax: +86-21-65985811; Tel: +86-21-65983292

substratum material is the basic problem of this system, and the interaction between algae cells and materials is worth further consideration. The answers to these questions will lay the theoretical foundation for the optimal selection of dielectric materials. The ideal material in large-scale cultures should have a small influence on algae, exhibit a good mass transfer effect, along with being simple to operate, durable and cost-effective. However, currently most of the used substratum materials are from the market, such as stainless steel, titanium plate, aluminum plate, plexiglass, plastic foam, micro polyethylene, nylon, polyester, cotton rope, newspaper, printing paper, *etc.*[12–16] The selection of materials depends entirely on experience or thorough evaluation from limited types of materials.

It should be noted that the algal properties, substratum properties, medium composition and hydrodynamic conditions are all factors that impact the algae attachment behavior.[8] Xia *et al.*[17] studied the surface properties of six algal species and found that all of the tested algae species were hydrophobic and tended to be electron donors. Shen *et al.*[18] compared nine commonly used materials and found that glass fiber-reinforced plastic was the optimal substrata. Hydrophobic properties, easy collection and durability were the three most important parameters determined by previous studies; however, having hydrophobic properties was not a universally accepted norm among all studies. Genin *et al.*[19] demonstrated that overall algal biofilm productivity was largely explained by differences in the colonization time which in turn was strongly correlated with the polar surface energy of the material and only weakly correlated with the water–material contact angle. This study also reported that the highest algae productivity was observed on cellulose acetate when compared with acrylic, glass, polycarbonate, and polystyrene. Full understanding of the adhesion mechanism could help explain how the relationship between the selection of algae and substratum impact the adhesion strength and thereby provide strategies for rational substratum selection in the market or through direct modification.[8]

This paper explores the selection of attached materials and the adherence characteristics of microalgae during the attached cultivation of microalgae. In this paper, *Chlorella pyrenoidosa*

was the selected microalgae. Five common microfiltration membranes, such as CA, polypropylene (PP) polyamides (PA), glass fiber (GF), and CA-CN membranes, were used as the supporting medium materials, and Basal (containing 1 g L^{-1} glucose) was used as the circulating fluid medium. First, the surface characteristics of microalgae and five dielectric materials were characterized. Second, the effects of different membrane materials on harvested biomass during attached cultivation were investigated. Finally, the thermodynamic mechanism of interaction between microalgae and different membrane materials was analyzed by XDLVO theory.

2 Materials and methods

2.1 Algae cultivation

The strain of *C. pyrenoidosa* (FACHB-9) was purchased from the Institute of Hydrobiology at the Chinese Academy of Sciences in China. Prior to being cultured in attached biofilm reactors, it was cultured in a sterilized Basal medium for two weeks under controlled ambient conditions at 25 ± 0.5 °C and a 14 h light/10 h dark cycle with illumination ranging from 2000 lx to 5000 lx over time (GZX-300BS-III, CIMO Co., Shanghai, China). To achieve a fast growth rate and a high productivity, 1.0 g L^{-1} of glucose was added into the medium. The medium consisted of KNO$_3$ (1250 mg L^{-1}), KH$_2$PO$_4$ (1250 mg L^{-1}), MgSO$_4$·7H$_2$O (1000 mg L^{-1}), EDTA (500 mg L^{-1}), H$_3$BO$_3$ (114.2 mg L^{-1}), CaCl$_2$·2H$_2$O (111 mg L^{-1}), FeSO$_4$·7H$_2$O (49.8 mg L^{-1}), ZnSO$_4$·7H$_2$O (88.2 mg L^{-1}), MnCl$_3$·4H$_2$O (14.2 mg L^{-1}), MoO$_3$ (7.1 mg L^{-1}), and CuSO$_4$·5H$_2$O (15.7 mg L^{-1}), Co (NO$_3$)$_3$·6H$_2$O (4.9 mg L^{-1}). The pH value was approximately 6.1. To prevent sedimentation of the algae, all conical flasks were placed on magnetic stirring plates (YG-60W, Fujian, China) and stirred at 250 rpm for 30 s twice per day.

2.2 Attached biofilm reactor

The attached biofilm reactor used in this study was a single layer attached photobioreactor (Fig. 1), which was utilized in a previous study.[20] As can be seen in Fig. 1, a 0.4 m × 0.2 m × 3 mm glass plate was placed in a 0.50 m × 0.30 m × 0.05 m
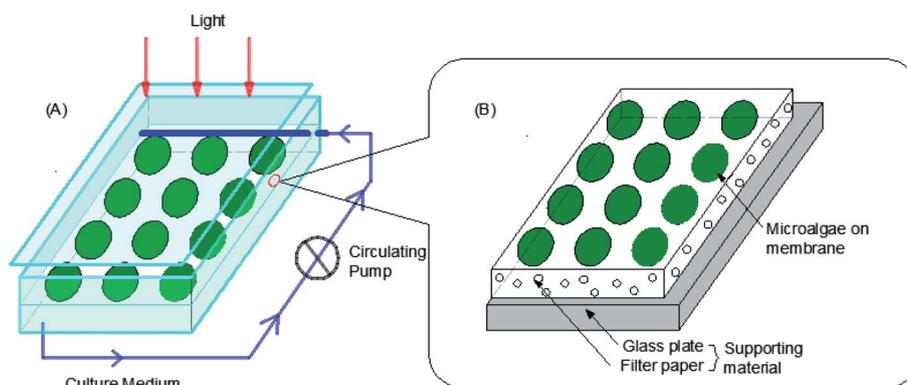

Fig. 1 A schematic diagram of the attached biofilm reactor. (A) The schematic diagram of the attached biofilm reactor with recycling of the culture medium. The medium was penetrated through the filter paper to the algae cells by a peristaltic pump when it flowed through the filter paper on the glass plate. (B) Detailed structure of the system's cultivation surface.

glass chamber at a certain angle. For easy sampling and measurement of the biomass, the microalgae cells were filtered on microfiltration membranes of different materials (Xingya Co., Shanghai, China, pore size = 0.45 μm) to form 'algae cakes' and then were attached to a filter paper on the glass plate. Each reactor could culture up to twelve 10 cm^2 size algae cakes. A circulatory pump (AT303S, Atman, Guangdong, China) was implemented inside the system. The Basal medium with 1.0 g L^{-1} glucose was uniformly penetrated into the filter paper by the pump to support the growth of microalgae. The flow rate was gently controlled at 60 mL h^{-1} to maintain the attachment of the algae cells with minimal wash-off. In addition, to ensure a stable environment and decrease evaporation loss in the culture medium, a large glass plate was placed to seal one side of the glass chamber. A fluorescent lamp was placed directly above the chamber which served as the light source, and the measured intensity at the position of algae was 60 ± 5 μmol (m^2 s)$^{-1}$. Other external culture conditions were the same as the liquid culture conditions of the algae species. The whole culture period was 8 days.

2.3 Algal biomass

The growth of microalgae was monitored by weighing the algal biomass harvested on the medium. The membranes with a certain thickness of algae were removed from the attached biofilm reactor, and the algae cells on the membrane were washed into a 50 mL centrifuge tube with a quantitative PBS buffer solution. After centrifugation, the supernatant was discarded, and the algae body was subsequently transferred to a weighed 10 mL centrifuge tube which was previously dried in a 60 °C oven until a constant weight was achieved. The constant weight of the centrifuge tube was W_1 (g). The dry weight of the dried tube with the algal body was W_2 (g), and W was the dry weight (g m^{-2}) of the algal cells on the membrane with the inoculation area A (m^2).

$$W \text{ (g m}^{-2}) = (W_2 - W_1)/A \qquad (1)$$

2.4 Contact angle

The contact angles of the membranes and algae were determined by a Dataphysics-OCA25 contact angle and surface free energy analyzer (Germany) based on the sessile-drop method. Before the measurement, the membranes were immersed in Milli-Q water for at least 48 hours and then placed in a freeze dryer. After freeze-drying for 24 h, the membranes were fixed onto the glass slide. De-ionized water, glycerol and diiodomethane were selected as the test titration liquids. Each sample was measured at least 5 times. Notably, the contact angle of the algae could not be detected until the algal cells completely covered the membrane surface and formed a distinct cake layer.[21]

2.5 Zeta potential

The zeta potential of the algal suspension was tested using a Malvern Zetasizer (Zetasizer Nano, England), while the zeta

potential of the algal suspension was tested using an Anton Paar Zetasizer (SurPass3, Austria) at a pH = 7.0. Each sample was measured in triplicate.

2.6 Roughness

The surface roughness of the five membrane materials was evaluated comprehensively by atomic force microscopy (AFM, Burker, Germany) and scanning electron microscopy (SEM, Phenom Pro, China). Before SEM was conducted, the freeze-dried samples were plated with gold and then scanned at an acceleration voltage of 30 kV. During the measurement process, the surface topography could not be measured by AFM due to the large surface roughness of the PP and GF membrane.

2.7 Surface free energy calculation

The surface free energy was calculated by determining the surface tension and the zeta potential. According to the extended version of Derjaguin Landau Verwey Overbeek (XDLVO) theory, when calculating the interaction energy, besides the Lifshitz–van der Waals force (LW), the electrostatic force (EL) interaction energy, and the acid–base (AB) interaction energy all cannot be ignored. Thus, the surface free energy was calculated as follows:[22,23]

$$\Delta G^{\text{TOT}} = \Delta G^{\text{LW}} + \Delta G^{\text{EL}} + \Delta G^{\text{AB}} \qquad (2)$$

where ΔG^{TOT} is the total interaction energy across the membrane; ΔG^{LW}, ΔG^{EL} and ΔG^{AB} are the Lifshitz–van der Waals force, the electrostatic force, and the acid–base interaction surface energy per unit area, respectively, which can be calculated as follows:[24]

$$\Delta G_{\text{awm}}^{\text{LW}} = 2\left(\sqrt{\gamma_{\text{w}}^{\text{LW}}} - \sqrt{\gamma_{\text{m}}^{\text{LW}}}\right)\left(\sqrt{\gamma_{\text{a}}^{\text{LW}}} - \sqrt{\gamma_{\text{w}}^{\text{LW}}}\right) \qquad (3)$$

$$\Delta G_{\text{awm}}^{\text{AB}} = 2\sqrt{\gamma_{\text{w}}^{+}}\left(\sqrt{\gamma_{\text{m}}^{-}} + \sqrt{\gamma_{\text{a}}^{-}} - \sqrt{\gamma_{\text{w}}^{-}}\right) + 2\sqrt{\gamma_{\text{w}}^{-}}\left(\sqrt{\gamma_{\text{m}}^{+}} + \sqrt{\gamma_{\text{a}}^{+}} - \sqrt{\gamma_{\text{w}}^{+}}\right) - 2\left(\sqrt{\gamma_{\text{m}}^{+}\gamma_{\text{a}}^{-}} + \sqrt{\gamma_{\text{m}}^{-}\gamma_{\text{a}}^{+}}\right)$$

$$(4)$$

$$\Delta G_{\text{awm}}^{\text{EL}} = \frac{\kappa \varepsilon_{\text{r}}\varepsilon_0}{2}\left(\zeta_{\text{m}}^2 + \zeta_{\text{a}}^2\right) \times \left(1 - \coth(\kappa y_0) + \frac{2\zeta_{\text{m}}\zeta_{\text{a}}}{\zeta_{\text{m}}^2 + \zeta_{\text{a}}^2} \operatorname{csch}(\kappa y_0)\right) \qquad (5)$$

where the subscripts a, w and m, represent the algae, water, and membrane, respectively; $\varepsilon_{\text{r}}\varepsilon_0$ is the dielectric permittivity of the fluid; ζ_{m} and ζ_{a} are the surface potentials of the membrane and the algae, respectively; κ is the inverse Debye screening length; and y_0 is the minimum equilibrium cut-off distance (0.157 nm (±0.009 nm)).[24] γ^{LW}, the electron-donating energy (γ^-) and the electron-accepting energy (γ^+) are calculated according to Young's equation.[25]

Moreover, the contribution of electrostatic force energy was small relative to the other surface energy components in the calculation. Therefore, the EL force energy was ignored to

simplify the analysis of the attached culture process in this study.

The equations of the above three forces are as follows:

$$F_{LW} = 2\pi y_0^2 \Delta G_{mlp}^{LW} r_p \left(\frac{1}{y^2}\right)\left(1 + \frac{5.32y}{\lambda_{LW}}\right)^{-1} \quad (6)$$

$$F_{AB} = 2\pi \Delta G_{mlp}^{AB} r_p \exp\left(-\frac{y_0 - y}{\lambda_{AB}}\right) \quad (7)$$

$$F_{EL} = 2\pi r_p \kappa \varepsilon_r \varepsilon_0 \left(\zeta_m^2 + \zeta_p^2\right) \times \left(\frac{2\zeta_m\zeta_p}{\zeta_m^2 + \zeta_p^2} - e^{-\kappa y}\right)\left(\frac{e^{-\kappa y}}{1 - e^{-2\kappa y}}\right) \quad (8)$$

3 Results and discussion

3.1 Effect of surface topography and roughness

According to a previous study, the adsorption density of algae cells is positively correlated with the surface roughness of certain materials.[26] In other words, algae cells are more likely to attach to materials with a rougher surface. Thus, the roughness of the five kinds of membranes in this study were evaluated. As shown in Table 1, the surface and 3D morphology of CACN, CA and PA membranes were observed by AFM, and the corresponding R_q (ratios of surface roughness) was obtained. There were uniform capillary micropores on the surface of CACN, CA and PA membranes, which were smooth and flat. Additionally, the surface roughness value of the PA membrane was higher than that of the CACN and CA membranes. The PP and GF membranes were only characterized by SEM images because they were too rough to scratch the AFM probe. The SEM images showed that the GF membrane clearly exhibited a loose, porous, fibrous structure with good gas permeability, which was beneficial for transporting CO_2 gas through the pores. The structure of the PP membrane was similar to the GF membrane, but the fiber distribution was free of GF membrane disorder. Hence, the roughness value of the PP membrane was also lower than that of the GF membrane. Furthermore, surface fractal dimension can be employed to describe the roughness of surface structure of membrane and the fractal dimension might be positively correlated with the roughness of the membrane surface.[27,28] The modeled three-dimensional (3D) fractal membrane surfaces of the PP and GF are displayed in Fig. S1 (ESI†). The fractal dimensions of the PP and GF are 2.316 and 2.4497, respectively, suggesting that the roughness of the GF was higher than that of PP. In summary, the roughness of the five materials determined *via* AFM and SEM results followed the trend (from high to low surface roughness value): GF > PP > PA > CACN > CA. Observing the membrane surface after attached cultivation, there was only a small difference between the membrane surface and the algae cake layer, indicating the microalgae grew well and evenly, and a certain thickness of algae cake layer completely covered the pores of the membrane.

In order to improve the efficiency of attached cultivation, more microalgae should be attached to the membranes to increase the light utilization rate and thereby enhance biomass accumulation. However, as the attached culture adopted an adsorption-type immobilization culture method, the microns-sized and rapidly metabolizing microalgae cells were easily washed by the medium water flow. On the rough solid surface, there were many pores and cracks. The presence of the pores, seams and wall surfaces in the gap provided a larger area for the microalgae to attach, and the microalgae that attached to it could therefore be retained. The shielded locations reduced the erosion of the algae cells by the hydraulic shear of the flowing medium, creating relatively static hydrodynamic conditions for the algae cells.

However, it is worth noting that although more algae cells tend to attach to materials with a rougher surface, too high of a roughness value of the material surface will increase the difficulty of harvesting, especially for algae cells which remain in the surface gap. This may cause the harvested amount of microalgae to be lower than the actual amount of microalgae on the material surface, which could result in a large waste of algae obtained from the culture. Therefore, it is necessary to select the appropriate surface roughness of the material through experimentation in order to achieve the ultimate harvesting purpose of the attached culture.
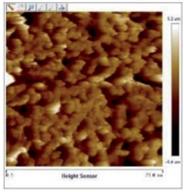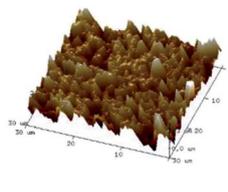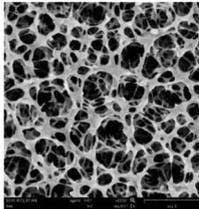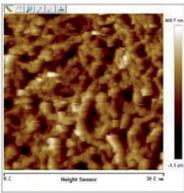
3.2 Biomass accumulation on different membrane surfaces

As shown in Fig. 2, the biomass that accumulated on the PP membrane was significantly lower than that of the other four membranes. During the experiment, it was found that the PP membrane was highly hydrophobic, resulting in its poor compatibility and adhesion characteristics with algae. Furthermore, due to PP's large surface roughness, the difficulty of harvesting increased, resulting in the biomass harvested on day 2 being even lower than day 0. It implied that the m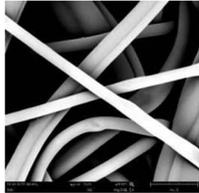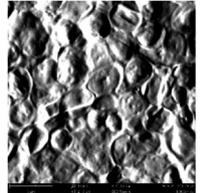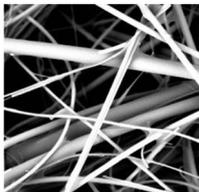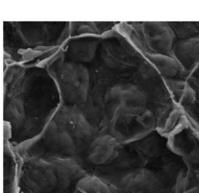icroalgae cells could be embedded in the surface gap of the PP membrane, leading to the difficulty of harvesting. Observing the biomass accumulation trend for each membrane, it can be seen that the PA membrane showed a sharp drop in the harvested biomass accumulation in the late stage of the culture, which was mainly related to the properties of the nylon membrane itself.

The swelling properties of PA membrane in wet or liquid environments have been reported in the previous studies.[29–31] The small-molecules interior of the PA membrane can cause the increase of the polymer chains and subsequently the change of the system's volume.[32] Furthermore, a large amount of small-molecules can result in the deterioration of the material's stability and subsequently caused swelling of the material when the culture period was long, and even destroy the original membrane structure.[32] Due to the presence of some non-crystalline polyamide polar genes in the nylon materials, there were large molecular weight amide-containing compounds in this part of the amorphous polyamide, which could be correlated with the presence of highly polar water molecules. This may have caused the deterioration of the material's stability and subsequently caused swelling of the material when the culture period was long. As a result, the mechanical strength was too low on the eighth day of the culture, and the membrane was

Table 1 Surface topographies and ratios of surface roughness (R_q) of the substrata[a]

Material/R_q (µm)	AFM surface characterization	AFM 3D characterization	SEM surface characterization	SEM surface characterization after cultivation
CACN/0.355				
CA/0.291				
PA/0.373				
PP	—	—		
GF	—	—		
Chlorella pyrenoidosa	—	—		
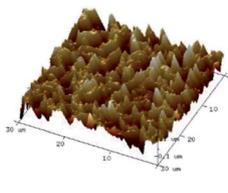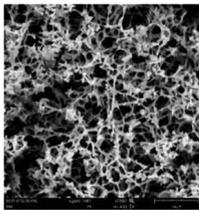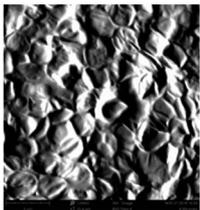
[a] Note: the scale bars are 6 µm and 5 µm in AFM and SEM, respectively.

broken which caused an increase in the loss of the harvested algal cells, thus the biomass obtained drastically reduced.

3.3 Free energy analysis between the membrane and microalgae

Table 2 lists the average contact angles of five pure membranes and algae measured by a contact angle meter. The contact angle

of the pure water reflected the degree of wetting of the membrane surface or algae cake layer, *i.e.*, the hydrophilicity of the membrane. A smaller contact angle reflected stronger hydrophilicity. It could be seen that among the 5 membrane materials, except for the PP membrane which was more hydrophobic and the CACN membrane which was weakly hydrophobic, the other membranes were all hydrophilic. In
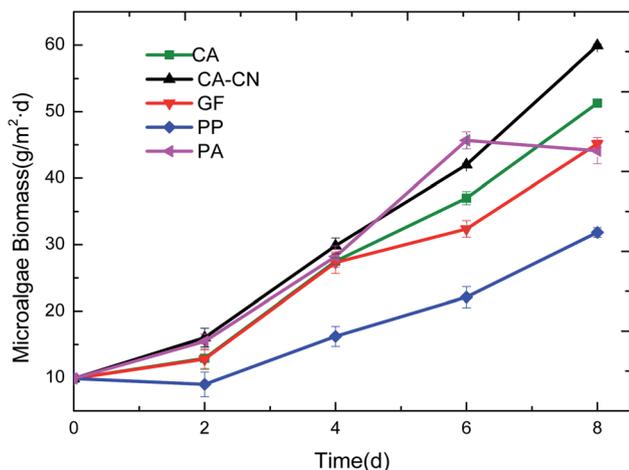
Fig. 2 Growth curves of *C. pyrenoidosa* on different membranes during attached cultivation.

particular, the GF membrane was notably more hydrophilic than the other membranes, because it could be completely wetted and therefore its hydrophilicity was too high to be determined numerically. In summary, the hydrophilicity of the five microfiltration membranes followed the order (from most hydrophilic to least hydrophilic): GF > PA > CA > CACN > PP. The angle of the algae was 92.14°, showing a significant hydrophobic tendency.

Table 3 and 4 show the surface tension and free energy parameters of the microalgae and the five membranes, respectively. It could be seen that the surface tension parameter was calculated by measuring the contact angle of the three reference liquids on each solid sample. The cohesion free energy of the polymerization of algae itself, the membrane itself (ΔG_{131}^{CO}) and the adhesion free energy for the adhesion between the algae and membrane (ΔG_{131}^{AD}) were calculated according to eqn (2)–(4).

The surface tension parameters of the six samples were analyzed first. The γ^- value reflected the ability of water molecules to form hydrogen bonds with the surface of the membrane material, which was greatly affected by the contact angle of the pure water. A higher γ^- value meaned greater attraction between the water molecules and the membrane material. Conversely, a lower γ^- value reflects lower gravitational force between the water molecules and the membrane, and the molecules other than water in the solution are more likely to accumulate on the membrane surface. The increase of the γ^-

value could increase the value of ΔG^{AB}, which determines the total surface free energy. The γ^{LW} value was related to the contact angle of diiodomethane. When the contact angle of diiodomethane was large, the γ^{LW} becomes smaller and thus increases the adhesion free energy.

As shown in Table 3, the adhesion free energy ΔG_{131}^{CO} reflected the ability of the substance's self-coagulation capacity, so it could indicate the thermodynamic stability (hydrophobicity) of a substance when it was immersed in water. When the ΔG_{131}^{CO} value was negative, the greater the absolute value, the more unstable the substance is in water, which showed that it tended to aggregate and was more hydrophobic. According to the calculation, the adhesion free energy of Chlorella was negative, indicating that it was more hydrophobic. The results also demonstrated that the algae particles tended to agglomerate and that the algae cake layer was dense. The free energy parameters of the polymerization can also verify the hydrophobicity of the membrane. As can be seen from Table 3, the adhesion free energy of polymerization of the 5 membranes was ranked according to the absolute value (from largest to smallest): GF > CA > CA-CN > PA > PP membrane; the hydrophilic order was also nearly the same (from largest to smallest): GF > PA > CA > CA-CN > PP.

The analysis of the two components ΔG_{131}^{LW} and ΔG_{131}^{LW} of the adhesion free energy ΔG_{131}^{CO} showed that ΔG_{131}^{LW}, the van der Waals effect of algae, was negative, indicating that there was always an attraction between the algae particles when they aggregated. ΔG_{131}^{AB}, the Levi's acid–base effect, was also negative, indicating that the algae particles were more attractive when they were close to each other, probably because of the polar –OH, COOH and –NH$_2$ functional groups which existed on the surface of the microalgae cells.[33] Due to the presence of these two forces, algae cells could accumulate with each other by eliminating the interference of the aqueous solution outside the particles. In addition to the PP membrane, the contribution of the van der Waals effect and Levi's acid–base effect to the total adhesion free energy (absolute value) was: $\Delta G_{131}^{AB} > \Delta G_{131}^{LW}$ (except for the PP membrane), which indicated that in the aqueous system, the algae–algae and membrane–membrane stability and polymerization ability were mainly affected by the Levi's acid–base effect of the organic matter, *i.e.*, the hydrophobic interaction force.

As shown in Table 4, the adhesion free energy (ΔG_{132}^{AD}) could indicate the strength of the interaction between the microalgae and the membrane surface during the process when algae

Table 2 Contact angles of the membranes and *Chlorella pyrenoidosa*

Entry	Sample	Contact angle (°)		
		θ_{wat}	θ_{gly}	θ_{dii}
1	CA	83.5 (±0.61)	67.67 (±0.22)	15.18 (±0.50)
2	CACN	96.34 (±0.79)	55.35 (±0.63)	14.09 (±0.98)
3	PP	130.57 (±1.33)	122.89 (±2.84)	14.66 (±0.13)
4	PA	62.38 (±2.31)	61.99 (±2.73)	12.72 (±0.37)
5	GF	—	143.9 (±2.73)	—
6	*Chlorella pyrenoidosa*	92.14 (±4.04)	68.70 (±2.40)	44.30 (±1.52)

Table 3 Cohesion free energy of the membranes and microalgae

Entry	Sample	Surface tension parameter					Free energy		
		γ^{LW}	γ^-	γ^+	γ^{AB}	γ^{TOT}	ΔG_{131}^{LW}	ΔG_{131}^{AB}	ΔG_{131}^{CO}
1	CA	49.04	2.26	0.00	0.14	49.18	−10.90	−70.99	−81.89
2	CA-CN	49.28	3.10	3.38	−6.47	42.82	−11.06	−42.27	−53.33
3	PP	49.16	0.45	21.47	−6.22	42.94	−10.97	−7.28	−18.25
4	PA	49.56	19.34	0.13	−3.14	46.42	−11.24	−12.23	−23.47
5	GF	50.80	285.89	82.47	−307.10	−256.30	−12.09	−191.24	−203.33
6	*Chlorella pyrenoidosa*	37.63	0.08	0.97	0.54	38.17	−4.29	−77.65	−81.95

Table 4 Adhesion free energy (ΔG_{132}^{AD}, mJ m^{-2}) between the membrane and microalgae

Entry	Sample	Free energy		
		ΔG_{132}^{LW}	ΔG_{132}^{AB}	ΔG_{132}^{AD}
1	CA	−10.90	−70.99	−81.89
2	CA-CN	−11.06	−42.27	−53.33
3	PP	−10.97	−7.28	−18.25
4	PA	−11.24	−12.23	−23.47
5	GF	—	—	—

particles approach the surface. When the ΔG_{132}^{AD} value was negative, the larger absolute value indicated a greater interaction strength, which signified that microalgae were more likely to be trapped on the membrane surface or secretions were more likely to be blocked inside the membrane pore to form irreversible adhesion. The calculation results in Table 4 indicated that there was a certain adhesion between algae and the 5 membranes. The order of adhesion free energy was (from highest to lowest) CA > CACN > PA > PP, which was basically the same as the order of biomass accumulation (from highest to lowest): CACN > CA > PA > PP.

The adhesion free energy, ΔG_{132}^{AD}, between the CA, CACN membrane and the Chlorella was obviously more negative than the PP and PA membranes, indicating that the interaction force between the two membranes and the algae was stronger, and algae cells were easier to adhere to the membrane to form an irreversible adhesion. This signified that more algal cells were able to stably adhere to the membrane surface for attached growth. It was speculated that this adhesion may be the main reason why the CA membrane and the CA-CN membrane were the preferred membranes for biomass accumulation. However, this theory relies too much on the data of the contact angle values. Some materials cannot be explained by this theory because it is difficult to obtain the contact angle.

3.4 Force analysis between microalgae and the CA-CN membrane

As shown in Fig. 3, taking the CA-CN membrane as an example, the F_{XDLVO} curve was calculated when the microalgae particles were close to the CA-CN membrane. F_{XDLVO} is the sum of the three forces F_{LW}, F_{AB} and F_{EL}. During the calculation process, the experimental parameters were as follows: the average radius

of the microalgae was 2 μm; the zeta potential of *C. pyrenoidosa* was −13.5 mV; and the zeta potential of the CA-CN membrane was 55.81 mV.

In this study, a positive force represented repulsion and a negative force represented attraction. As can be seen from Fig. 3, under the action of kinetics, the microalgae particles began to approach the surface of the CA-CN membrane. When there was a large distance between the two particles, the force was very close to zero. When the distance between the particles reached above 16 nm, up to the surface of the membrane, the F_{EL} started to increase. The F_{EL} value was always positive, verifying the theory that electrostatic interaction was a repulsive force that prevented the microalgae from approaching the membrane surface. When the algae–membrane distance was between 6 nm and 16 nm, F_{EL} played a dominant role, and F_{AB} and F_{LW} were both negligible because the values of these forces were small. From a distance of 6 nm to the membrane surface, it could be seen that the two force curves of F_{AB} and F_{LW} increased rapidly, and the rate of increase of F_{AB} was much larger than that of F_{LW}. The F_{LW} value was negative, which verified that the van der Waals force was attractive in the theory; the F_{AB} was negative, which indicated that the Levis acid–base force also showed gravitation in this system. Under these three forces, F_{XDLVO} exhibited repulsive force from a distance to 4.6 nmThe repulsion of F_{XDLVO} peaked at approximately 6 nm (0.296 nN).
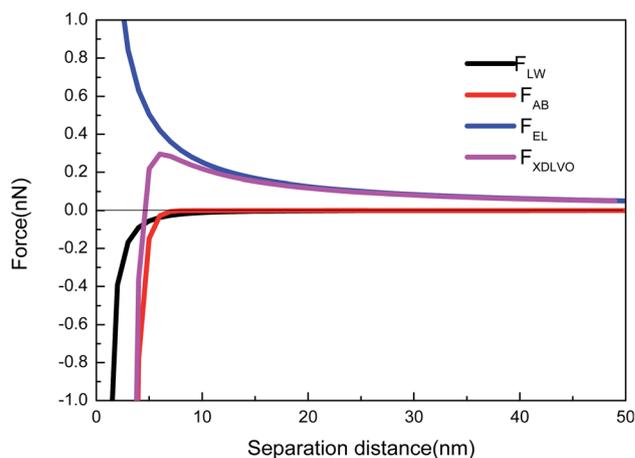
Fig. 3 XDLVO force profiles when microalgae approached the CA-CN membrane.

However, F_{XDLVO} showed a gravitational effect within 4.6 nm of the microalgae, and F_{XDLVO} increased rapidly as the distance increased. When the microalgae attached to the membrane, that is, when the distance was $y = 0.16$ nm, the FEL, FAB, FLW and FXDLVO values were 15.77, −468, −67.31 and −533.41 nN, respectively. It is apparent that when the microalgae completely attached to the membrane surface, FEL was negligible compared with the sum of FAB and FLW. This also verified the rationality of ignoring the electrostatic interaction and only adopting the van der Waals interaction energy and the Levi's acid–base energy when calculating the surface free energy.

4 Conclusion

C. pyrenoidosa is a hydrophobic algae which tended to agglomerate, indicating that a dense algae layer was formed. Moreover, the membrane's cohesion free energy was mutually verifiable with its hydrophobicity. The Levi acid and alkali played a major role in quantifying this energy value, which always behaved in an attractive manner. The adhesion free energy between the microalgae and the membrane verified the accumulation of biomass in this study. Comparing the two free energies, the former was significantly larger than the latter, which led to the adhesion of more microalgae to the membrane during the adherence process. The XDLVO theory can be used to simulate the relationship between the force of the algae membrane and the distance when the microalgae approaches the membrane surface during attached cultivation.

Author contributions

Yonggang Zhang conceptualized the project, discussed the results, as well as wrote and revised the manuscript. Rui Ma completed formal analysis, investigation and characterization techniques, as well as wrote and revised the manuscript. Huaqiang Chu discussed the results and wrote and revised the manuscript. Xuefei Zhou discussed the results and wrote and revised the manuscript. Tianming Yao conceptualized the project and designed the work, as well as wrote and revised the manuscript. Yalei Zhang conceptualized the project and designed the work, as well as wrote and revised the manuscript.

Conflicts of interest

There was no conflict to declare.

Acknowledgements

References

1 A. L. Gonçalves, J. C. M. Pires and M. Simões, *Environ. Chem. Lett.*, 2013, **11**, 315–324.

2 D. Vandamme, I. Foubert and K. Muylaert, *Trends Biotechnol.*, 2013, **31**, 233–239.

3 T. M. Mata, A. A. Martins and N. S. Caetano, *Renewable Sustainable Energy Rev.*, 2010, **14**, 217–232.

4 T. Cai, S. Y. Park and Y. Li, *Renewable Sustainable Energy Rev.*, 2013, **19**, 360–369.

5 J. J. Milledge and S. Heaven, *Rev. Environ. Sci. Bio/Technol.*, 2013, **12**, 165–178.

6 P. Wang, J. L. Li, X. Q. Luo, M. Ahmad, L. Duan, L. Z. Yin, B. Z. Fang, S. H. Li, Y. Yang, L. Jiang and W. J. Li, *Funct. Ecol.*, 2021, DOI: 10.1111/1365-2435.13949.

7 M. Gross, D. Jarboe and Z. Wen, *Appl. Microbiol. Biotechnol.*, 2015, **99**, 5781–5789.

8 T. Liu, J. Wang, Q. Hu, P. Cheng, B. Ji, J. Liu, Y. Chen, W. Zhang, X. Chen and L. Chen, *Bioresour. Technol.*, 2013, **127**, 216–222.

9 F. Berner, K. Heimann and M. Sheehan, *J. Appl. Phycol.*, 2015, **27**, 1793–1804.

10 J. Wang, W. Liu and T. Liu, *Bioresour. Technol.*, 2017, **244**, 1245–1253.

11 C. Ji, J. Wang, R. Li, T. Liu, C. Ji, J. Wang, R. Li and T. Liu, *Bioproc. Biosyst. Eng.*, 2017, **40**, 1079–1090.

12 A. Ozkan, K. Kinney, L. Katz and H. Berberoglu, *Bioresour. Technol.*, 2012, **114**, 542–548.

13 W. Blanken, M. Janssen, M. Cuaresma, Z. Libor, T. Bhaiji and R. Wijffels, *Biotechnol. Bioeng.*, 2014, **111**, 2436–2445.

14 H. C. Bernstein, M. Kesaano, K. Moll, T. Smith, R. Gerlach, R. P. Carlson, C. D. Miller, B. M. Peyton, K. E. Cooksey and R. D. Gardner, *Bioresour. Technol.*, 2014, **156**, 206–215.

15 T. Naumann, B. R. Podola and M. Melkonian, *J. Appl. Phycol.*, 2013, **25**, 1413–1420.

16 S. G. Vasilieva, E. S. Lobakova, A. A. Lukyanov and A. E. Solovchenko, *Moscow Univ. Biol. Sci. Bull.*, 2016, **71**, 170–176.

17 L. Xia, H. Li and S. Song, *J. Appl. Phycol.*, 2016, **28**, 2323–2332.

18 Y. Shen, X. Xu, Y. Zhao and X. Lin, *Bioproc. Biosyst. Eng.*, 2014, **37**, 441–450.

19 S. N. Genin, J. S. Aitchison and D. G. Allen, *Bioresour. Technol.*, 2014, **155**, 136–143.

20 P. Cheng, J. Wang and T. Liu, *Bioresour. Technol.*, 2015, **185**, 527–533.

21 L. A. Ahmad, M. H. N. Yasin, C. J. C. Derek and K. J. Lim, *J. Membr. Sci.*, 2013, **446**, 341–349.

22 E. M. Hoek and G. K. Agarwal, *J. Colloid Interface Sci.*, 2006, **298**, 50–58.

23 L. Li, Z. Wang, L. C. Rietveld, N. Gao, J. Hu, D. Yin and S. Yu, *Environ. Sci. Technol.*, 2014, **48**, 14549–14557.

24 J. A. Brant and A. E. Childress.

25 Y. D. Shikhmurzaev, *Phys. Lett. A*, 2008, **372**, 704–707.

26 N. J. Hallab, K. J. Bundy, K. O'Connor, R. L. Moses and J. J. Jacobs, *Tissue Eng.*, 2001, **7**, 55–71.

27 A. Adeniyi, R. Mbaya, P. Popoola, F. Gomotsegang, I. Ibrahim and M. Onyango, *Alexandria Eng. J.*, 2020, **59**, 4397–4407.

28 Q. Wei and D. Wang, *Mater. Lett.*, 2003, **57**, 2015–2020.

29 E. Drazevic, K. Kosutic and V. Freger, *Water Res.*, 2014, **49**, 444–452.

30 V. Freger, *Environ. Sci. Technol.*, 2004, **38**(11), 3168–3175.

31 E. P. Chan, A. P. Young, J.-H. Lee, J. Y. Chung and C. M. Stafford, *J. Polym. Sci., Part B: Polym. Phys.*, 2013, **51**, 385–391.

32 S. Wang, K. Gu, J. Wang, Y. Zhou and C. Gao, *J. Membr. Sci.*, 2019, **575**, 191–199.

33 W. Stumm and J. J. Morgan, *Aquatic chemistry: chemical equilibria and rates in natural waters*, John Wiley & Sons, 2012.